

# A novel algorithm for ocean wave direction inversion from X-band radar images based on optical flow method

WANG Li<sup>1</sup>, CHENG Yunfei<sup>1\*</sup>, HONG Lijuan<sup>1</sup>, LIU Xinyu<sup>1</sup>

<sup>1</sup>Third Research Institute, Ministry of Public Security, Shanghai 200031, China

Received 11 May 2017; accepted 15 June 2017

©The Chinese Society of Oceanography and Springer-Verlag GmbH Germany, part of Springer Nature 2018

## Abstract

As one of the important sea state parameters for navigation safety and coastal resource management, the ocean wave direction represents the propagation direction of the wave. A novel algorithm based on an optical flow method is developed for the ocean wave direction inversion of the ocean wave fields imaged by the X-band radar continuously. The proposed algorithm utilizes the echo images received by the X-band wave monitoring radar to estimate the optical flow motion, and then the actual wave propagation direction can be obtained by taking a weighted average of the motion vector for each pixel. Compared with the traditional ocean wave direction inversion method based on frequency-domain, the novel algorithm is fully using a time-domain signal processing method without determination of a current velocity and a modulation transfer function (MTF). In the meantime, the novel algorithm is simple, efficient and there is no need to do something more complicated here. Compared with traditional ocean wave direction inversion method, the ocean wave direction of derived by using this proposed method matches well with that measured by an *in situ* buoy nearby and the simulation data. These promising results demonstrate the efficiency and accuracy of the algorithm proposed in the paper.

**Key words:** X-band radar, optical flow, weighted average, ocean wave direction, radar image

**Citation:** Wang Li, Cheng Yunfei, Hong Lijuan, Liu Xinyu. 2018. A novel algorithm for ocean wave direction inversion from X-band radar images based on optical flow method. Acta Oceanologica Sinica, 37(3): 88–93, doi: 10.1007/s13131-018-1201-9

## 1 Introduction

The state of ocean wave is regarded as the focal point of ocean research, which is closely related to human beings activities. For now, the ocean wave is an important and meaningful ocean environment parameter. It has significant meaning for shore protection, ocean development, ocean environmental protection, and ocean military affairs. Sea state parameters such as wave height, wave period, and wave direction are numerical information which have a direct link to the wave motion. As one of the important sea state parameters for a navigation safety and a coastal resource management, the ocean wave direction represents the propagation direction of the wave. The monitoring of the sea state by a X-band radar is of timely interest because this kind of radar gives the opportunity to scan the sea surface with high temporal and spatial resolutions under various sea conditions in the near range ( $\geq 5$  km) of the X-band radar (Young et al., 1985; Senet et al., 2008). The X-band radar echo signal is usually displayed as gray-level image sequences. By analyzing these image sequences, spectral characteristics corresponding to sea surface dynamics (ocean wave directions for example) can be found (Wang et al., 2015).

At present, the retrieval of the ocean wave direction from marine X-band radar image sequences is usually based on a wave number spectrum (Huang et al., 2014). While the wave number spectrum can be obtained in the following way, Young et al. (1985) uses the 3-D fast Fourier transform (FFT) of the radar image sequences in Cartesian coordinates to extract an image

spectrum. The rectangular temporal sequence of consecutive radar images of the sea surface acquired by an X-band wave monitoring radar system is  $E(x, y, t)$ . The time interval between two consecutive images is  $\Delta t$ . The spatial resolutions  $\Delta x$  and  $\Delta y$  of each image are dependent on an azimuthal resolution due to the effective aperture of the antenna and on a range resolution due to the radar pulse length. Then the rectangular temporal sequence is transformed into the spectral domain by means of a FFT to estimate the so-called image spectrum  $F_i(\vec{k}, \omega)$ . The signals of sea waves are located along a surface in the wave number frequency domain defined by the dispersion relation of linear surface-gravity waves. The surface connects the wave numbers  $\vec{k}$  with their corresponding frequency coordinate  $\omega$ . The dispersion relation has the following formula:

$$\omega(\vec{k}) = \sqrt{g|\vec{k}| \tanh(|\vec{k}|h) + \vec{k}\vec{u}}, \quad (1)$$

where  $\omega(\vec{k})$  indicates the angular frequency;  $g$  is the gravitational acceleration;  $h$  is the water depth;  $\vec{k}$  is the wave number; and  $\vec{u}$  is the current velocity of encounter, which is a sum of the platform velocity and the near-surface current velocity (Wang et al., 2016).

The sea surface current which extracted from the image spectrum by an iterative least squares method from the dispersion re-

Foundation item: The National Key Research and Development Program of China under contract No. 2016YFC0800405; the Shanghai Municipal Science and Technology Project of China under contract No. 15DZ0500600; the Specialized Research Fund for the Doctoral Program of Higher Education of China under contract No. 2014212020203.

\*Corresponding author, E-mail: zou2013@whu.edu.cn

lation (1) is used to construct a band-pass filter to separate the energy associated with the ocean waves from a background noise and to remove those components of the image spectrum which do not belong to the wave field (Vicen-Bueno et al., 2012). The filtered three-dimensional image spectrum is denoted as  $F_i(\vec{k}, \omega)$  and the wave propagation direction function can be obtained from the wave spectrum by using a transform function defined by

$$D(f, \theta) = \frac{F_i(\vec{k}, \omega) |M(\vec{k})|^{-2}}{S(f)}, \quad (2)$$

where  $S(f)$  is the frequency spectrum; and  $|M(\vec{k})|^2$  is a modulation transfer function determined by

$$|M(\vec{k})|^2 = F_i(\vec{k}) / F_i(\vec{k}) \propto |\vec{k}|^\beta, \quad (3)$$

where  $F_i(\vec{k})$  is the one-dimensional wave number spectrum derived from the radar measurements;  $F_i(\vec{k})$  is the corresponding spectrum derived from the frequency spectrum  $S(f)$  obtained from heave time series measured by *in situ* sensors. According to the results of the forefathers, usually  $\beta=1.2$  (Gangeskar, 2002).

Without the accurate measurement result of current, there will be serious bias in the wave propagation direction inversion due to the erroneous calculation of the band-pass filter (Senet et al., 2001). What is more, the modulation transfer function (MTF) estimation always contains error ineluctably due to the limit of data, measurement, instrumental, computational, and even human errors, which in turn have an effect on the selecting of the MTF for the wave propagation direction inversion. To avoid the impact of inaccurate current and to reduce the error, proceeding from the radar signals in the time domain, a novel algorithm based on the optical flow method is developed for ocean wave direction inversion of the ocean wave fields. The proposed algorithm utilizes the echo images received by the X-band wave monitoring radar to estimate the optical flow motion efficiently and simply, and then the actual wave propagation direction can be obtained by taking a weighted average of the motion vector for each pixel.

## 2 Ocean wave direction inversion algorithm

### 2.1 Optical flow method

The sequences of ordered images allow the estimation of motion as either instantaneous image velocities or discrete image displacements (Beauchemin and Barron, 1995). Fleet and Weiss provide a tutorial introduction to gradient-based optical flow. John L (Brox and Malik, 2011). Barron et al. (1994) provide a performance analysis of a number of optical flow technologies. It emphasizes the accuracy and density of measurements. An optical flow method is an excellent way to analyze the moving objects from the image sequence. As a simple and practical engineering application approach to estimate the motion vectors of the image gray-scale, the optical flow method can detect moving objects in radar sequence images with complex background clutters. An optical flow field is a collection of all the optical flow points, also known as image motion field and image velocity field, it contains the rich information of target movement and brightness change. Therefore, the movement of all image pixels can be obtained by the optical flow.

At present, the optical flow motion estimation technologies to approximate motion field is based on the change in the time domain and the correlation of a pixel intensity in the image sequence. It describes the relationship between the gray change and the movement of the gray in the image. The core of the optical flow method is the speed of the target and the movement of objective object is relatively continuous, so the pixels projected on the plane of a sensor or a receiving device are continuously changing too. For this reason, we can assume that the instantaneous grey value remains the same according to a region brightness invariant theory and the flow constraint equation (Bung and Valero, 2016) can be obtained by

$$I(x, y, t) = I(x + dx, y + dy, t + dt), \quad (4)$$

where  $I(x, y, t)$  is the gray-scale of pixel  $(x, y)$  at time  $t$ . Decomposing the right-hand side of the equality by use of Taylor series expansion, we have

$$I(x + dx, y + dy, t + dt) = I(x, y, t) + \frac{\partial I}{\partial x} dx + \frac{\partial I}{\partial y} dy + \frac{\partial I}{\partial t} dt. \quad (5)$$

Then the change rate of the gray-scale with respect to time can be obtained by the space grade of the gray-scale dot product the speed from Eqs (4) and (5):

$$\frac{\partial I}{\partial x} u + \frac{\partial I}{\partial y} v = -\frac{\partial I}{\partial t}, \quad (6)$$

where  $\vec{u} = (u, v)$ , is the velocity vector of the pixel;  $u = \frac{dx}{dt}$ ; and  $v = \frac{dy}{dt}$ . From Eq. (6) we have

$$\begin{bmatrix} \frac{\partial I}{\partial x} & \frac{\partial I}{\partial y} \end{bmatrix} \begin{bmatrix} u \\ v \end{bmatrix} = -\frac{\partial I}{\partial t}, \quad (7)$$

assuming that  $A\vec{u} = b$ ,  $A = \begin{bmatrix} \frac{\partial I}{\partial x} & \frac{\partial I}{\partial y} \end{bmatrix}$  and  $b = -\frac{\partial I}{\partial t}$ , then the final computation results of the velocity vector of the pixel can be obtained by calculating the velocity vector with the minimum value of  $\|A\vec{u} - b\|^2$  based on the least square method and the optical flow method:

$$\vec{u} = (A^T A)^{-1} A^T b. \quad (8)$$

### 2.2 Ocean wave direction inversion

The sea surface waves are mechanical waves that propagate along the interface between water and air, the restoring force is provided by the gravity, and so they are often referred to as surface gravity waves. As the wind blows, a pressure and a friction perturb the equilibrium of the water surface and transfer energy from the air to the water, forming waves. Ocean waves have a certain amount of randomness and they can be described as a stochastic process (Donelan et al., 1992). What is more, it is generally considered that the research of the ocean waves can be simplified based on the statistic stationary random process theory during the observation period. In the imaging process of the

X-band radar, the positions of the bright-dark stripes in conjoint sea clutter images will have deviation over time. Since the deviation is mainly caused by the periodic movement of the ocean wave, the deviation direction is the propagation direction of the wave.

The ocean wave direction will remain basically unchanged during collection of serial echo images and the radar echo images basically meet the three elements of the optical flow: velocity field ocean wave movement, the part containing the movement information such as gray-scale pixels and the projection from the ocean wave to the plane of radar image. For this reason, we can obtain the motion vector set  $\vec{u} = (u, v)$  of every pixel in the image sequence within a period of time by applying the optical flow method to the radar echo image sequence directly. The motion vector of every pixel in the image sequence is composed of speed  $|\vec{u}|$  and direction  $\theta$ . The speed  $|\vec{u}|$  represents the size of the offset of pixel point and the offset will be larger when the direction of pixel point is the same with the wave propagation direction. In order to use the speed and direction of the estimated motion vector together wisely and efficiently to improving the accuracy of measuring results, by using the speed of the pixel point as the weights assigned to the directions of all the pixel points, we can obtain the optimal direction of the wave propagation finally. The direction of the wave propagation calculation has the following expression:

$$\theta = \frac{\sum_{i=1}^n |\vec{u}_i| \theta_i}{\sum_{i=1}^n |\vec{u}_i|}, \quad (9)$$

where  $\theta$  is the direction of wave propagation;  $\theta_i$  and  $|\vec{u}_i|$  are the velocity and direction of the  $i$ th pixel point, respectively; and  $n$  is the number of all the pixel points in the radar image sequence. In order to verify the novel algorithm for the ocean wave direction inversion from the X-band radar images based on the optical flow method developed in this paper, the simulation data and the field collecting data are used for the wave direction inverting based on Eq. (9).

### 3 Numerical simulation

#### 3.1 Ocean wave simulation

Although the waving of the ocean wave is not a strictly stationary and absolutely regular process, the wave motion within a short time can be regarded as a kind of quasi stationary process. According to Longuet-Higgins (1957) sea wave model, the ocean waves can be considered as composed result of sinusoidal waves with different amplitudes, frequencies and phases:

$$\eta(x, y, t) = \sum_{n=1}^{\infty} a_n \cos[\omega_n t - k_n (x \cos \theta_n + y \sin \theta_n) + \varepsilon_n], \quad (10)$$

where  $a_n$  is the wave amplitude;  $\omega_n$  is the angular frequency;  $\varepsilon_n$  is the initial phase;  $k_n$  is the wave number of  $n$ th sinusoidal wave; and  $\theta_n$  is the direction of the wave propagation,  $-\pi \leq \theta_n \leq \pi$ .

The frequency-direction wave spectrum is the product of a frequency spectrum and a direction factor (Hasselmann et al., 1980; Hanson and Phillips, 1999):

$$S(f, \theta) = S(f)G(f, \theta), \quad (11)$$

where  $G(f, \theta)$  is the direction function. Since the stormy waves in different growth phases can be described by JONSWAP wave spectrum, we use the JONSWAP wave spectrum for the ocean wave simulation (Kitaigorodskii et al., 1975). The formula of the JONSWAP is

$$S(f) = \alpha \frac{g^2}{4\pi^2 f^5} \times \exp \left[ -\frac{5}{4} \left( \frac{f}{f_p} \right)^4 \right] \gamma^{\exp \left( -\frac{(f-f_p)^2}{2\sigma^2 f_p^2} \right)}, \quad (12)$$

where  $\gamma$  is a peak enhancement factor;  $\sigma$  is a spectral width parameter; and the scale factor  $\alpha$  and the peak frequency  $f_p$  can be computed directly by the wind speed and the wind area. What is more, the direction function  $G(f, \theta)$  used in the ocean wave simulation is commonly from stereo wave observation project (SWOP) (Chase et al., 1957):

$$G(f, \theta) = \frac{1}{\pi} (1 + a \cos 2\theta + b \cos 4\theta), \quad (13)$$

$$\begin{cases} a = 0.5 + 0.82 \exp \left[ -\frac{1}{2} \left( \frac{f_p}{f} \right)^4 \right], \\ b = 0.32 \exp \left[ -\frac{1}{2} \left( \frac{f_p}{f} \right)^4 \right]. \end{cases} \quad (14)$$

The wave amplitude  $a_n$  is defined as follows:

$$a_n = \sqrt{2S(\omega_n, \theta_n) \Delta \omega \Delta \theta}. \quad (15)$$

Bringing Eq. (15) into Longuet-Higgins sea wave model, we can simulate a series of ocean waves with different propagation directions. The frequency-direction wave spectrum based on the JONSWAP wave spectrum with the wave direction of dominant energy at an angle of 45 is shown in Fig. 1.

#### 3.2 Analysis and comparisons of simulation results

The simulation radar echo image with the wind speed around 10 m from the sea surface is 12 m/s, the length of a wind area is 12 km and the wave direction of the dominant energy at an angle of 45 is shown in Fig. 2a. As shown in Fig. 1, the gray scale corresponds to the radar backscatter strength, pixels on the images

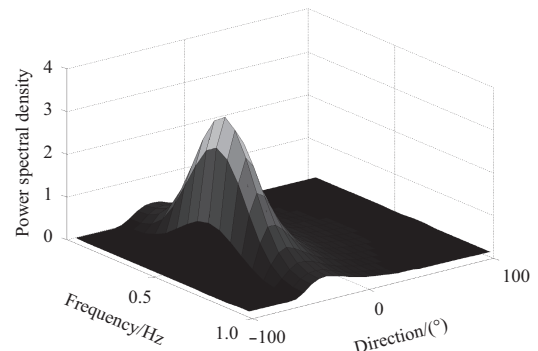
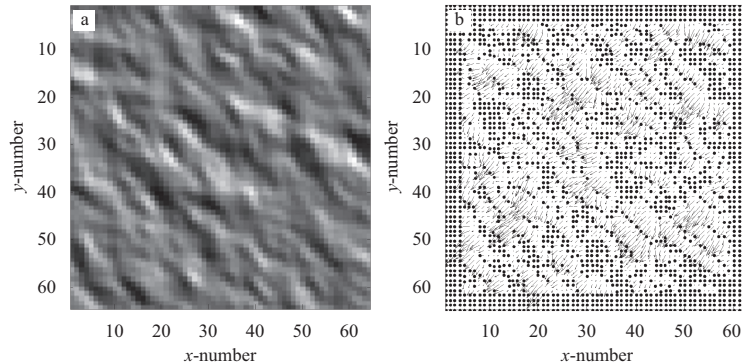


Fig. 1. The simulation of the frequency-direction wave spectrum.



**Fig. 2.** The simulation radar echo image with the wave direction of the dominant energy at an angle of  $45^\circ$  (a) and the motion vector set of every pixel in the image by applying the optical flow method to the radar echo image sequence (b).

with a resolution of 7.5 m in range and the image includes  $128 \times 128$  pixel points. The Gaussian noise with the signal to noise ratio (SNR) is 10 dB and the influence of shadow modulation is considered in the simulation, the rotation speed of the antenna is 60 r/min and the height of the antenna is 50 m. The closest distance between the image and the radar station is 2 000 m.

The motion vector set of every pixel in the image by applying the optical flow method to the radar echo image sequence directly is shown in Fig. 2b. The arrows in the image represent the speed and direction of the pixels. As there are 64 frames in an image sequence, we can obtain the motion vector field of each image. Thus the ocean wave direction can be estimated by substituting the motion vectors of all the pixels into Eq. (9).

To know if the proposed ocean wave direction estimating algorithm given by this paper is a good approach to estimate the ocean wave direction, it is necessary to carry out comparisons between the ocean wave direction values derived from the simulated image sequences of the ocean waves with different propagation directions by the proposed method and the setting values. The scatter plots of the two kinds of ocean wave direction are shown in Fig. 3, the ocean wave directions are uniformly scattered within  $0^\circ$ – $350^\circ$  and the number of the simulation data is 71. A root-mean-square error (RMSE) and correlation coefficient ( $r$ ) for them are  $6.1^\circ$  and 0.98, which show that the ocean wave direction retrieved correlates well with the setting values and have the same tendency.

#### 4 Experimental results

To further make sure about the effect of the approach to estimate the ocean wave direction in this paper, it is necessary to carry out comparisons between the ocean wave direction values derived from a reference measuring sensor and the ocean wave direction values estimated by the proposed method. The ocean wave direction data used for verification of the presented algorithm were obtained during January 8, 2014 to January 10, 2014, by the X-band wave monitoring radar. The radar is a kind of marine monitoring instrument refitted from a navigation radar and its operating frequency is X-band  $[(9\ 410 \pm 30)\text{ MHz}]$ . Under the ocean wave observation mode, its performance parameters are: its antenna dimension is less than 2.438 4 m at a rotation speed of 42 r/min, horizontal polarization, and the transmitting power is 12 kW, its pulse width is 0.05  $\mu\text{s}$ , a pulse repetition is 3 000 Hz, the maximal detection range is 5 km, the radial range resolution is 7.5 m and the directional resolution is approximately  $0.95^\circ$  (Wang et al., 2016b).

The testing site is located at Zhoushan City, Zhejiang

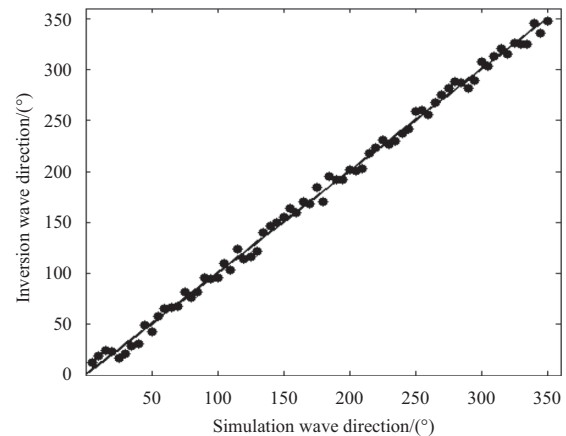


**Fig. 3.** The scatter plots of the two kinds of ocean wave direction.

Province, China. The X-band radar station was mounted on top of a hill which is about 70 m above the sea level and 100 m from the coastline. The west of the radar station is land, and the east of it is the sea. The average depth of the observation area is 50 m. At 1 000 m away from the radar station in the azimuth of  $140^\circ$ , an *in situ* wave buoy (SZF2-1A) is placed for comparison. As the buoy worked every 30 min, the radar was set the same to the buoy. Locations of the experiment site and sensors are shown in Fig. 4.

The image sequence collected by the X-band radar contains 128 images and each frame includes  $128 \times 128$  pixel points. The size of each pixel point is 7.5 m  $\times$  7.5 m and the size of observation area is 960 m  $\times$  960 m. A single measured radar echo image and the motion vector set of every pixel in an image by applying the optical flow method to the radar echo image sequence is shown in Fig. 5.

For the duration of the experiment, the comparison of the ocean wave direction derived from marine X-band radar image sequences and those measured by the buoy is shown in Figs 6–7 and Table 1. To validate the proposed method, these results are compared with the ocean wave direction which is calculated by the traditional ocean wave direction estimation algorithm. The time series of the three kinds of ocean wave direction are shown in Fig. 6 and the results show that the ocean wave direction estimated by the proposed method is comparable with that estimated by the traditional method, and both of them match well with that measured by the buoy.

The scatter plots of ocean wave direction measured by the buoy are compared to that estimated by our proposed method in



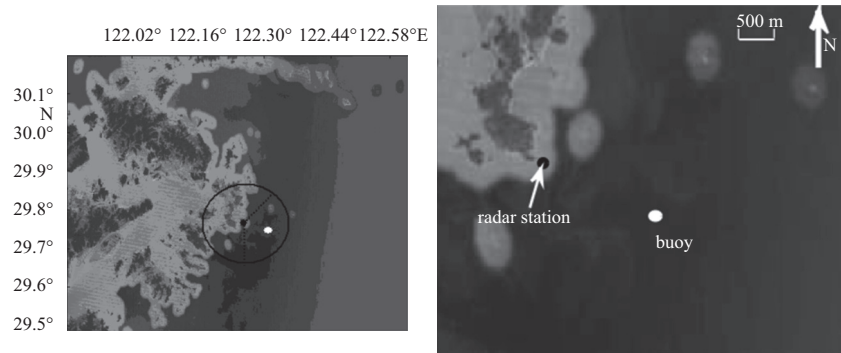


**Fig. 4.** Map of the experiment site. Locations of the radar station and buoy are shown by the white and black dots respectively, and a harbor lies on the west of the area. The black solid circle denotes the FOV of the radar, and the radar station lies in the center of the circle, and the two dashed lines denote the sea in the radar FOV.

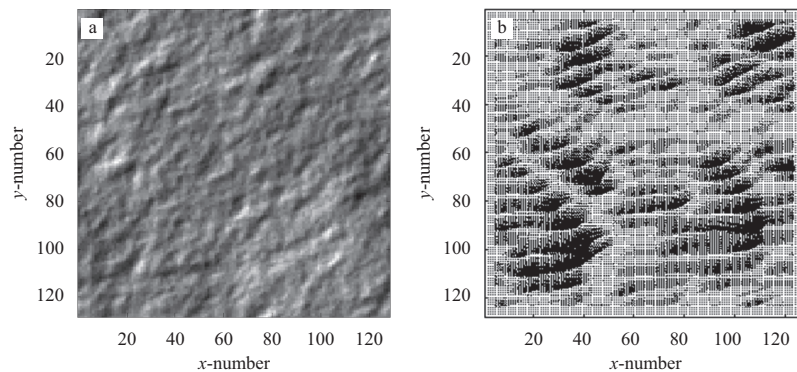


**Fig. 5.** The measured radar echo image (a) and the motion vector set of every pixel in the image by applying the optical flow method to the radar echo image sequence (b).

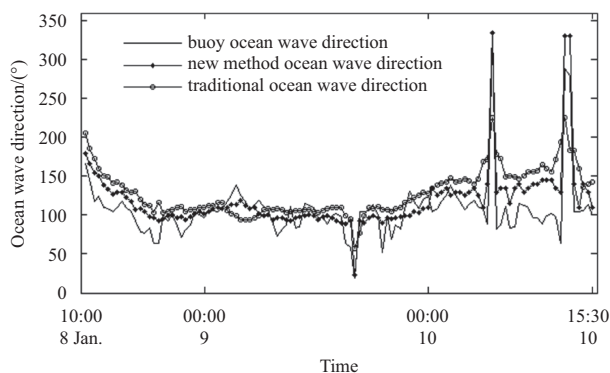


**Fig. 6.** Time series of ocean wave direction during the experiment.

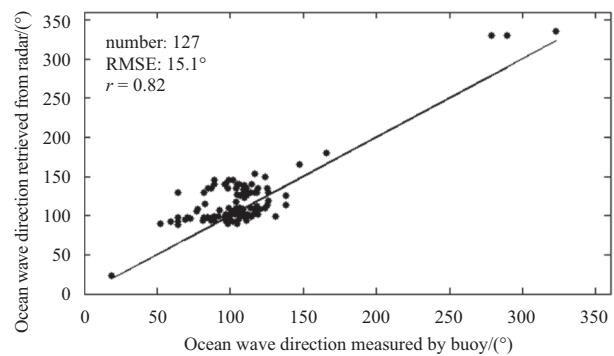


**Fig. 7.** Scatter plots of the ocean wave direction measured by the buoy and that retrieved from marine X-band radar image sequences by using the proposed method.

**Fig. 7.** The root-mean-square error (RMSE), bias, and correlation coefficient ( $r$ ) for them are 15.1°, 9.8° and 0.82, which show that the ocean wave direction retrieved correlates well with the in situ measurements. **Table 1** reports the performances in terms of the RMSE, bias, and  $r$  for the traditional and the new method to estimate ocean wave direction. It is evident that the results of the proposed method match the measurement of the buoy better than, at least as well as the traditional method.

## 5 Conclusions

This paper presents a novel approach to estimate the ocean wave direction from X-band radar images, and the validation of

**Table 1.** Comparison of the derived ocean wave directions from the traditional method and the new method.

	RMSE/(°)	Bias/(°)	$r$
Traditional method	22.1	12.6	0.75
New method	15.1	9.8	0.82

this method by comparing with the simulation data according to the JONSWAP wave spectrum and the observations of a buoy nearby. The novel algorithm is fully based on the optical flow method to extract the movement information of pixels from radar signals in the time domain without the determination of current

velocity and MTF. The validation proves that the novel algorithm provides the ocean wave direction with accuracy rate amount to 82%. It provides new insights into the motion estimation of pixels for the ocean wave direction inversion from X-band radar images easily and efficiently. Our future work will include doing more experiments under different sea states and experiment platforms such as moving vessels and extending the algorithm to obtain more wave parameters which are theoretically feasible to be used in the ocean wave direction.

## References

- Barron J L, Fleet D J, Beauchemin S S. 1994. Performance of optical flow techniques. *International Journal of Computer Vision*, 12(1): 43–77
- Beauchemin S S, Barron J L. 1995. The computation of optical flow. *ACM Computing Surveys*, 27(3): 433–466
- Brox T, Malik J. 2011. Large displacement optical flow: descriptor matching in variational motion estimation. *IEEE Transactions on Pattern Analysis and Machine Intelligence*, 33(3): 500–513
- Bung D B, Valero D. 2016. Optical flow estimation in aerated flows. *Journal of Hydraulic Research*, 54(5): 575–580
- Chase J, Cote L J, Marks W, et al. 1957. The Directional Spectrum of a Wind Generated Sea as Determined from Data Obtained by the Stereo Wave Observation Project. *IEEE International Conference on Communications*, : 5274–5280
- Donelan M, Skafel M, Graber H, et al. 1992. On the growth rate of wind-generated waves. *Atmosphere-Ocean*, 30(3): 457–478
- Gangeskar R. 2002. Ocean current estimated from X-band radar sea surface, images. *IEEE Transactions on Geoscience and Remote Sensing*, 40(4): 783–792
- Hanson J L, Phillips O M. 1999. Wind sea growth and dissipation in the open ocean. *Journal of Physical Oceanography*, 29(8): 1633–1648
- Hasselmann D E, Dunckel M, Ewing J A. 1980. Directional wave spectra observed during JONSWAP 1973. *Journal of Physical Oceanography*, 10(8): 1264–1280
- Huang Weimin, Gill E, An Jiaqi. 2014. Iterative least-squares-based wave measurement using X-band nautical radar. *IET Radar, Sonar & Navigation*, 8(8): 853–863
- Kitaigorodskii S A, Krasitskii V P, Zaslavskii M M. 1975. On Phillips' theory of equilibrium range in the spectra of wind-generated gravity waves. *Journal of Physical Oceanography*, 5(3): 410–420
- Longuet-Higgins M S. 1957. Statistical properties of an isotropic random surface. *Philosophical Transactions of the Royal Society: A. Mathematical, Physical and Engineering Sciences*, 250(975): 157–174
- Senet C M, Seemann J, Flampouris S, et al. 2008. Determination of bathymetric and current maps by the method DISC based on the analysis of nautical X-band radar image sequences of the sea surface (November 2007). *IEEE Transactions on Geoscience and Remote Sensing*, 46(8): 2267–2279
- Senet C M, Seemann J, Ziemer F. 2001. The near-surface current velocity determined from image sequences of the sea surface. *IEEE Transactions on Geoscience and Remote Sensing*, 39(3): 492–505
- Vicen-Bueno R, Lido-Muela C, Nieto-Borge J C. 2012. Estimate of significant wave height from non-coherent marine radar images by multilayer perceptrons. *EURASIP Journal on Advances in Signal Processing*, 2012(1): 84
- Wang Li, Wu Xiongbin, Ma Ketao, et al. 2016a. Elimination of the impact of vessels on ocean wave height inversion with X-band wave monitoring radar. *Chinese Journal of Oceanology and Limnology*, 34(5): 1114–1121
- Wang Li, Wu Xiongbin, Pi Xiaoshan, et al. 2015. Numerical simulation and inversion of offshore area depth based on X-band microwave radar. *Acta Oceanologica Sinica*, 34(3): 108–114
- Wang Li, Wu Xiongbin, Yue Xianchang, et al. 2016b. A novel algorithm in estimating signal-to-noise ratio for ocean wave height inversion from X-band radar images. *IEEE Geoscience and Remote Sensing Letters*, 13(3): 344–348
- Young I R, Rosenthal W, Ziemer F. 1985. A three-dimensional analysis of marine radar images for the determination of ocean wave directionality and surface currents. *Journal of Geophysical Research*, 90(C1): 1049–1059